Mamba State-Space Models Are Lyapunov-Stable Learners

Anonymous authors
Paper under double-blind review

Abstract

Compute-efficient methods–e.g., mixed-precision fine-tuning (MPFT) and parameter-efficient fine-tuning (PEFT)–have become standard tools for Transformer-based large language models (LLMs). While near-ubiquitously adapted, we empirically show that under different combinations of MPFT and PEFT, Transformer LLMs may drastically diverge from their respective full-precision counterparts. In stark contrast, we show that recent Mamba LLMs (Gu & Dao, 2024a; Dao & Gu, 2024) based on state-space models (SSMs) are significantly more stable to changes introduced by combinations of MPFT and PEFT. This robustness is due to the recurrent dynamics of Mamba SSMs, which we prove are guaranteed to be stable using dynamical systems theory (in particular, Lyapunov exponents). Additionally, we demonstrate how targeting different Mamba parameters for low-rank adaptation provides regularization and impacts PEFT generalization. We conclude by using MPFT and PEFT to novelly study Mamba LLMs' in-context learning (ICL) abilities on *natural language tasks*, thus supplementing other recent work.

1 Introduction

Upon their introduction in Gu & Dao (2024a), Mamba state-space models (SSMs) were shown to greatly outperform comparable attention-based LLMs (Biderman et al., 2023) across a large number of standard natural language benchmarks. Subsequently, pretrained Mamba models have been widely adapted across a large number of data modalities (Liu et al., 2024; Li & Chen, 2024; Quan & Li, 2024; Li et al., 2024), tasks (Xie et al., 2024; Wang et al., 2024a), and architectures (Anthony et al., 2024; Park et al., 2024; Lieber et al., 2024). Despite such widespread adaptation and subsequent research threads (Dao & Gu, 2024; Park et al., 2024; Wang et al., 2024b), no existing work has sought to understand the stability of learning Mamba SSMs in common LLM fine-tuning frameworks, such as mixed-precision fine-tuning (MPFT).

For recurrent-based deep models, such as Mamba SSMs, the sensitivity of recurrent dynamics to small changes (e.g., those introduced by mixed-precision) is a primary concern for stable learning (Bengio et al., 1994; Pascanu et al., 2013). While prior works have established the stability of previous SSM architectures (Goel et al., 2022; Orvieto et al., 2023), these results critically rely on the *time-invariance* property of the underlying state-space equations. For Mamba models–the major innovation of which are *time-varying* state-space parameters–prior stability results are not applicable.

To determine the stability of time-varying Mamba models, we leverage theory from dynamical systems. Deriving and bounding the Lyapunov exponents for both Mamba and Mamba-2 models, we show that small input changes within the SSM layer of either model do not lead to exponentially deviating outputs. Empirically, we validate this theoretical result; compared to full-precision fine-tuning, deviations due to MPFT are significantly more stable than those of comparable Transformers (Section 3). Furthermore, this trend continues **when MPFT and PEFT are combined**, where **Mamba SSMs** again **produce significantly smaller deviations compared to comparable Transformer LLMs**.

Our stability experiments also uncover that, unlike Mamba LLMs, Transformer-based LLMs trained under different combinations of MPFT and PEFT may drastically differ from their full-precision full fine-tuning counterparts, exhibiting what we call *large deviation spikes*. Over two widely used fine-tuning datasets and two widely used natural language benchmarks, attention-based LLMs Pythia (Biderman et al., 2023) and

OpenELM (Mehta et al., 2024) exhibit 9 and 4 large deviation spikes, respectively, whereas Mamba LLMs exhibit zero.

For PEFT via Low Rank Adaptation (LoRA) (Hu et al., 2021), we empirically demonstrate that Mamba models are robust to the choice of fine-tuning hyperparameters. Evaluating 150 hyperparameter configurations, Mamba models display a maximum performance difference of 1.5%, compared to 4.7% for comparable Transformers (Section 3.1). Additionally, we show that LoRA targeting a specific linear layer in Mamba models simultaneously regularizes parameters via weight tying while providing PEFT. For Mamba-2 models, **adapting this linear layer yields better performance on 32 of 35 experiments**, compared to adapting other linear layers.

Finally, we use stable MPFT and PEFT to explore the ICL capabilities of instruction tuned Mamba and Mamba-2 models on *natural language tasks*, thus complementing recent studies which evaluated Mamba ICL on synthetic tasks (Park et al., 2024; Lee et al., 2024). While the ICL capabilities of pretrained Mamba models lag behind those of comparable Transformer models–Mamba and Mamba-2 models only achieve 38% and 82%, respectively, of the performance improvements (relative to zero-shot) of Pythia models–instruction tuned Mamba-1 and Mamba-2 models improve to 81.5% and 132% of the ICL improvements achieved by Pythia.

Our major contributions are summarized as follows:

- We derive bounds on the Lyapunov exponents of both Mamba and Mamba-2 models' SSM equations. Using these bounds, we theoretically show that small input changes within the SSM layer do not lead to exponentially deviating outputs.
- Empirically, we extensively demonstrate the above theoretical result; across two fine-tuning datasets, two widely used natural language benchmarks, several model sizes, and a large number of MPFT/PEFT configurations, we show that training Mamba LLMs is significantly more stable than comparable Transformer-based LLMs.
- Using stable MPFT and PEFT, we complement recent studies by examining the ICL capabilities of Mamba/Mamba-2 models evaluated on *natural language tasks.* We show that instruction tuning allows SSMs to perform ICL competitively with comparable Transformer LLMs on natural language tasks.

Terminology. When describing a particular foundation model or result, we use the term “Mamba model” to refer to one of the original models released in Gu & Dao (2024a) and “Mamba-2 model” to refer to models released in Gu & Dao (2024a). Despite subtle architectural differences, these two SSMs share the same state-space equations and design scheme of storing the majority of SSM parameters in a large memory buffer. We thus synonymously use the term `MambaBlock` to refer to the SSM layer of both Mamba and Mamba-2 models.

2 Mamba state-space models

For latent-variable dimension d and maximum input sequence length T, the `MambaBlock` defines state-space parameters $\mathbf{A}, \mathbf{B}_t, \mathbf{C}_t, \mathbf{\Delta}_t \in \mathbb{R}^{d \times d}$ for $t \in \{1, \ldots, T\}$. The matrix $\mathbf{\Delta}_t$ controls the discrete step-size. Given an input sequence $\mathbf{u}_1, \ldots, \mathbf{u}_T \in \mathbb{R}^d$, the following linear mapping through latent states $\boldsymbol{x}_1, \ldots, \boldsymbol{x}_T \in \mathbb{R}^d$ is used to produce the output $\mathbf{y}_1, \ldots, \mathbf{y}_T \in \mathbb{R}^d$:

$$\boldsymbol{x}_t = \bar{\mathbf{A}}_t \boldsymbol{x}_{t-1} + \bar{\mathbf{B}}_t \mathbf{u}_t \tag{1}$$

$$\mathbf{y}_t = \mathbf{C}_t \boldsymbol{x}_t, \tag{2}$$

where $\bar{\mathbf{\Delta}}_t = \texttt{softplus}(\texttt{Linear}(\mathbf{\Delta}_t)) \in \mathbb{R}^{d \times d}$, $\bar{\mathbf{A}}_t = \exp(\bar{\mathbf{\Delta}}_t \mathbf{A})$ and $\bar{\mathbf{B}}_t = \mathbf{A}^{-1}(\bar{\mathbf{A}} - \mathbf{I})\mathbf{B}_t$. In practice, $\mathbf{A}, \mathbf{B}_t, \mathbf{C}_t$ and $\mathbf{\Delta}_t$ are diagonal matrices.

Due to the time-variance of Equations 1 and 2, previous SSM stability results are no longer applicable (discussed further in Appendix D). The Mamba foundation models were pretrained in full `FP32` precision and, subsequently, official implementations have cautioned against training in reduced precision (Gu & Dao, 2024b; Huggingface, 2024). Thus, how sensitive the `MambaBlock`'s recurrent dynamics are remains an open question. We next answer the latter using theory from dynamical systems.

2.1 Stable dynamics in the `MambaBlock`

For Mamba's discrete dynamic system in Equations 1 and 2, define

$$\boldsymbol{x}_t = F_\theta(\boldsymbol{x}_{t-1}, \mathbf{u}_t), \tag{3}$$

where θ denotes the time-varying parameters described in Section 2. For input sequence $\mathbf{u}_1, \ldots, \mathbf{u}_T$ and initial latent state vector $\boldsymbol{x}_0$, we thus write

$$\boldsymbol{x}_T = F_\theta(F_\theta(\ldots F_\theta(\boldsymbol{x}_0, \mathbf{u}_1))) \coloneqq F_\theta^{T-1}(\boldsymbol{x}_0, \mathbf{u}_1).$$

The rate of divergence between two scalar ε-close inputs to a discrete dynamical system is bounded by the system's maximal Lyapunov exponent $\lambda_{\texttt{max}}$ (Mikhaeil et al., 2022). Given $\lambda_{\texttt{max}}$ and two initial values $(\boldsymbol{x}_0, \mathbf{u}_1)$ and $(\boldsymbol{x}_0 + \varepsilon, \mathbf{u}_1 + \varepsilon)$, the maximum deviation between these points grows as (Laffargue et al., 2013; Sayama, 2015):

$$\max |F_\theta^N(\boldsymbol{x}_0, \mathbf{u}_1) - F_\theta^N(\boldsymbol{x}_0 + \varepsilon, \mathbf{u}_1 + \varepsilon)| \in \mathcal{O}(\varepsilon \exp(N\lambda_{\texttt{max}})).$$

Thus, when $\lambda_{\texttt{max}} > 0$, nearby trajectories exponentially separate and, when $\lambda_{\texttt{max}} \leqslant 0$, nearby trajectories ultimately converge to the same fixed point or periodic cycles.

The maximal Lyapunov exponent is defined as

$$\lambda_{\texttt{max}} \coloneqq \lim_{T \to \infty} \frac{1}{T} \log \left\| \prod_{t=0}^{T} \frac{\partial \boldsymbol{x}_t}{\partial \boldsymbol{x}_{t-1}} \right\|_2,$$

where $\|\|_2$ denotes the spectral norm for matrices. For an arbitrary `MambaBlock`, we prove the following:

Theorem 1. *Let $(\boldsymbol{x}_{t-1}, \mathbf{u}_t)$ be the latent state and input at an arbitrary time $t \in \{1, \ldots, T\}$ within a `MambaBlock`. Then small changes $(\boldsymbol{x}_{t-1} + \varepsilon, \mathbf{u}_t + \varepsilon)$ produce deviations which are exponentially non-increasing over discrete-time. That is,* $\max |F_\theta^N(\boldsymbol{x}_{t-1}, \mathbf{u}_t) - F_\theta^N(\boldsymbol{x}_{t-1} + \varepsilon, \mathbf{u}_t + \varepsilon)| \in \mathcal{O}(\varepsilon \exp(N\zeta))$*, for some scalar $\zeta \leqslant 0$.*

The proof of Theorem 1 is available in Appendix A, where the maximal Lyapunov exponent for an arbitrary `MambaBlock` is first proven to be non-positive. The main result subsequently follows.

Thus, the latent states of Mamba and Mamba-2 models are stable under small input changes. However, variables $\mathbf{y}_1, \ldots, \mathbf{y}_T$ are the primary outputs for such models, particularly for LLM applications. We next show that, given Theorem 1, Mamba and Mamba-2 output variables are also stable.

Theorem 2. *Assume $(\boldsymbol{x}_{t-1} + \varepsilon, \mathbf{u}_t + \varepsilon)$ produce deviations which are exponentially non-increasing over discrete-time. Then small changes to the output $\mathbf{y}_t$ are also exponentially non-increasing over discrete time.*

The proof of Theorem 2 is available in Appendix B. Thus, by Theorems 1 and 2, the latent and output states of both Mamba and Mamba-2 models are stable to changes encountered during recurrency.

2.1.1 Consequences for automatic mixed-precision

During a forward pass, automatic mixed-precision (AMP) saves time and memory by computing forward activations in half-precision (`FP16` or `BF16`). During a backward pass, AMP computes gradients in half-precision and up-casts to full-precision prior to updating. In contrast to full-precision fine-tuning, MPFT within the `MambaBlock` thus results in small differences to the inputs $\mathbf{u}_1, \ldots, \mathbf{u}_T$ (which are passed through a `Swish`), $\bar{\mathbf{\Delta}}_t$ (which is passed through a `softplus`), and the gradients calculated during training.

For a discrete dynamical system with $\lambda_{\texttt{max}} > 0$, changes due to AMP compound after repeated expansion of the recurrent state, thus leading to exponential deviations between quantities calculated using mixed- versus full-precision. However, by Theorem 1, $\lambda_{\texttt{max}} \leqslant 0$ within the `MambaBlock`. Therefore, **differences introduced by AMP for Mamba models do not exponentially compound over discrete-time.**

2.2 Hardware-aware optimizations and PEFT

Primary contributions of both Mamba (Gu & Dao, 2024a) and Mamba-2 (Dao & Gu, 2024) were hardware-efficient implementations of Equations 1 and 2. The former introduced extensively customized CUDA kernels which accessed the majority of time-varying parameters through a large buffer of GPU memory. The latter similarly stores the majority time-varying parameters in a large GPU memory buffer, while leveraging semiseparable matrices to express Equation 2 using tensor contractions (which are natively optimized on modern hardware accelerators).

In both cases, the memory buffer $\mathbf{W} \in \mathbb{R}^{T \times 3d}$ is used to store and access the diagonal elements of $\mathbf{B}_t, \mathbf{C}_t$ and $\mathbf{\Delta}_t$ for all $t \in \{1, \ldots, T\}$, such that

$$\mathbf{W}[t-1, : d] = \mathtt{diag}(\mathbf{\Delta}_t), \tag{4}$$

$$\mathbf{W}[t-1, d : 2d] = \mathtt{diag}(\mathbf{B}_t), \tag{5}$$

$$\mathbf{W}[t-1, 2d : 3d] = \mathtt{diag}(\mathbf{C}_t), \tag{6}$$

$$\tag{7}$$

where $\mathbf{W}[0, : d] = \mathtt{diag}(\mathbf{\Delta}_1), \mathbf{W}[n-1, d : 2d] = \mathtt{diag}(\mathbf{B}_T)$, and so on. In practice, $\mathbf{W}$ is instantiated as a `PyTorch` linear layer's weight matrix. The importance of $\mathbf{W}$ for both Mamba and Mamba-2 models makes it a primary candidate for LoRA adaptation, where low-rank matrices are used to adapt the frozen weight matrices of targeted linear layers. In such cases, selecting $\mathbf{W}$ for LoRA adaptation results in the following:

Theorem 3. *Consider the weight matrix* $\mathbf{W}$ *of a* `MambaBlock` *from Equation 4. Targeting* $\mathbf{W}$ *for LoRA during fine-tuning ties adaptation weights across* $\mathbf{B}_t, \mathbf{C}_t$ *and* $\mathbf{\Delta}_t$.

The proof of Theorem 3 is available in Appendix C. Section 3.1 demonstrates targeting $\mathbf{W}$, versus other linear layers, improves performance across a large number of natural language tasks.

3 Experiments

We explore the implications of Theorem 1 on fine-tuning, wherein mixed-precision is especially critical; MPFT combined with PEFT adapters have been shown to drastically reduce Transformer fine-tuning times (Dettmers et al., 2024). We focus on utilizing LoRA (Hu et al., 2021), which is arguably the most widely used PEFT framework for LLMs. Using the `Alpaca` dataset (Taori et al., 2023), `Mamba 160M`, `410M`, and `790M` models are fine-tuned for three epochs with a maximum sequence length of 512. We denote the targeting of all linear layers (ALL) for LoRA as *ALL LoRA*, the targeting of a subset of linear layers (SLL) for LoRA as *SLL LoRA*, and no adapters as *Full* (i.e., full fine-tuning). Both `ALL` and `SLL LoRA` adapt the large memory buffer described in Theorem 3.

Each fine-tuning run occurred on a single Nvidia A10G GPU (24 GB total memory). To further limit extraneous numerical effects, the same batch size is used for all `FP32`, `FP16`, and `BF16` experiments for a given model size. While this leads to hardware underutilization (i.e., non-saturated GPU memory for mixed-precision and LoRA experiments), this is necessary to guarantee no divergence is due to differences in parameter update schedules. For comparison, two Transformer-based LLM families of similar parameter counts are fine-tuned using the same experimental setup: `Pythia` (sizes `160M`, `410M`, and `1B`) and `OpenELM` (Mehta et al., 2024) (sizes `270M` and `450M`). The training recipe for all models was adapted from (Tunstall et al., 2023), with the `AdamW_torch` optimizer and a `cosine annealing` schedule. Further experimental details are available in Appendix E.

All models were evaluated using the LM evaluation harness from Eleuther AI (Gao et al., 2023). **Model performance is measured as percent accuracy** using the MMLU (Hendrycks et al., 2020) and Winogrande (Sakaguchi et al., 2021) datasets. The difference in model performance is reported as the mean *divergence* (i.e., absolute difference) between the original full-precision and respective mixed-precision model, averaged over {0, 1, 3, 5}-shot percent accuracy. Thus, **a divergence greater than one denotes an average difference greater than one entire percentage of accuracy.** We thus refer to a divergence greater than unity as a *large deviation spike.*

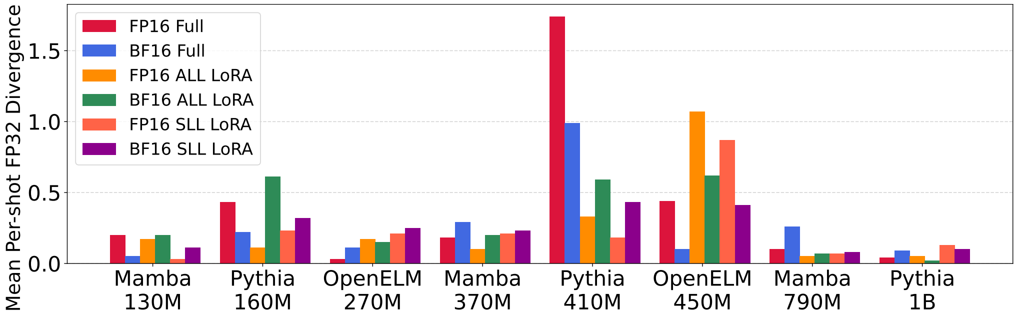

(a) Mean full-precision (`FP32`) divergence in MMLU performance.

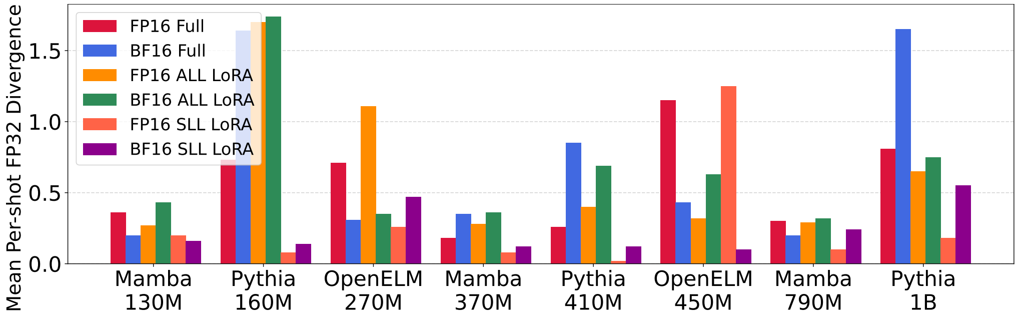

(b) Mean full-precision (`FP32`) divergence in Winogrande performance.

Figure 1: Mean full-precision (`FP32`) divergence in performance for Mamba, Pythia, and OpenELM models. Models are fine-tuned over the `Alpaca` dataset using different combinations of MPFT and PEFT. Full fine-tuning (i.e., no PEFT adapters) is denoted as `Full`.

Mean divergence results for all models are displayed in Figure 1(a) and Figure 1(b) for MMLU and Winogrande, respectively. Across mixed-precisions and adapter settings, Mamba displays smaller divergences than both Pythia and OpenELM models. E.g., **for Winogrande evaluations, `Alpaca` fine-tuning with Mamba models is an average 2.9 and 2.4 times smaller in mean divergence than Pythia and OpenELM models, respectively**. For MMLU evaluations, `Alpaca` fine-tuning with Mamba models is an average 2.6 times smaller in mean divergence than both Pythia and OpenELM models. Importantly, Mamba models do not exhibit large deviation spikes after fine-tuning, in contrast to both Pythia and OpenELM models.

We note that the results in Figure 1 display the fine-tuning of 72 LLMs and 576 few-shot evaluations. In Appendix G, these experiments are expanded to include the `LIMA` fine-tuning dataset (Zhou et al., 2024) as well as the standard deviations for all mean deviation results. Across all experiments, Mamba models are significantly more stable for MPFT/PEFT compared to Transformer-based LLMs. E.g., **for MMLU evaluations, `LIMA` fine-tuning with Mamba models is an average 7 and 3.3 times smaller in mean divergence than Pythia and OpenELM models, respectively**. For Winogrande evaluations, `LIMA` fine-tuning with Mamba models is an average 4.1 and 3.3 times smaller in mean divergence than Pythia and OpenELM models, respectively. **Across the two fine-tuning datasets, two benchmarks, and six evaluated MPFT/PEFT combinations, Pythia and OpenELM produce 9 and 4 large deviation spikes, respectively, while Mamba produces zero.**

3.1 Hyperparameter tuning robustness of Mamba models

We empirically demonstrate that Mamba models are robust to the choice of PEFT hyperparemters. Using the training recipe of Tunstall et al. (2023) as a basis, we conduct an extensive hyperparameter search across the learning rate, LoRA dimension, and number of warmup steps. From the Cartesian-product of these three parameters, 150 hyperparameter configurations were sampled and used to fine-tune `Mamba 370M` over the

Openhermes dataset (Teknium, 2024), which consists of 242,000 supervised samples. For comparison, `Pythia 410M` is similarly fine-tuned using the same set of 150 hyperparameter configurations.

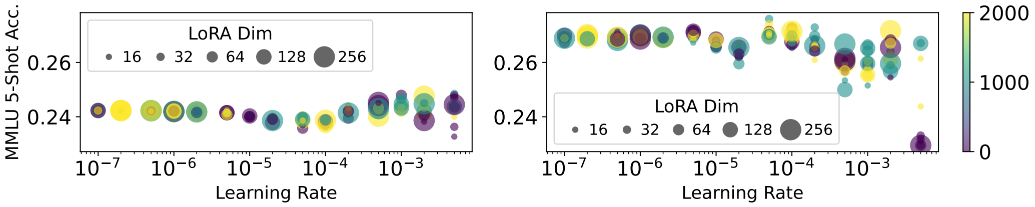

(a) `Mamba 370M` (b) `Pythia 410M`

Figure 2: Fine-tuning hyperparameter search for OpenHermes. Each point is a different hyperparameter configuration. `SLL LoRA` was used for both models. The x-axis is the learning rate, the y-axis is resulting MMLU 5-shot performance, bubble size is the LoRA dimension, and the color is the number of warmup steps $\in \{0, 1k, 2k\}$.

The MMLU 5-shot performance for each of the 150 Mamba and Pythia fine-tuned models is displayed in Figure 2. `Pythia 410M` is capable of higher performance than `Mamba 370M`, where the average accuracy for the former and the latter are 26.5% and 24.8%, respectively. However, `Mamba 370M` is much more robust to the choice of hyperparameters, with a difference of 1.5% between the minimum (23.3%) and maximum (24.8%). In contrast, `Pythia 410M` fine-tuned models display a large performance difference of 4.7% between the minimum (22.9%) and maximum (27.6%).

LoRA-layer robustness of Mamba models We next show that carefully targeting specific Mamba layers (Theorem 3) can lead to more effective learning. For PEFT via LoRA, we thus explore the impact of targeting $\mathbf{W}$ (i.e., the linear weight storing the majority of time-varying SSM parameters) on performance.

Using OpenHermes and the training recipe described in Section 3 (with `BF16`), we instruction tune Mamba-2 models using LoRA by both adapting $\mathbf{W}$ and adapting all linear layers other than $\mathbf{W}$. Zero-shot performance is evaluated using five standard natural language benchmarks: HellaSwag (Zellers et al., 2019), PIQA (Bisk et al., 2020), Arc-E (Clark et al., 2018), Arc-C (Clark et al., 2018), and WinoGrande (Sakaguchi et al., 2021). As shown in Appendix E.2 Table 4, PEFT with only $\mathbf{W}$ targeted near uniformly results in better performance than targeting other layers, with the former outperforming the latter on 32 out of 35 natural language tasks.

3.2 Stable instruction tuning improves Mamba ICL for natural language tasks

With both stable MPFT and PEFT, we determine the impact of instruction tuning Mamba and Mamba-2 models on ICL for natural language tasks. We instruction fine-tuned Mamba and Mamba-2 pretrained models using `ALL LoRA`, the OpenHermes, and the training recipe described in Section 3 (with `BF16`). Zero and few-shot performance are evaluated using the same five standard natural language benchmarks used in Section 3.1. ICL performance is reported as the *average improvement percentage* of {1, 3, 5}-*shot* versus 0-*shot* (AIPSS). For comparison, Pythia pretrained models are instruction fine-tuned using the same training recipe and `ALL LoRA` (i.e., all Pythia linear layers are adapted).

Figure 3 displays AIPSS for pretrained and instruction fine-tuned Mamba and Pythia models. As previously noted, pretrained Mamba models do not display similar ICL ability as comparable Pythia models on the evaluated standard NLP benchmarks. In particular, `Mamba 2.8B`, the largest pretrained Mamba model, displays inconsistent zero-shot improvements as the number of shots increase. While pretrained Mamba-2 models display significantly better ICL ability than Mamba models, Mamba-2 models smaller than 780 million parameters struggle.

However, after instruction tuning, all Mamba models larger than `Mamba 130M` consistently improve in ICL performance as the number of shots increase. Similarly, the majority of Mamba-2 models larger than `Mamba-2 130M` greatly improve in ICL performance. Thus, while pretrained Mamba and Mamba-2 models are only capable of 38% and 82% (respectively) of the AIPSS compared to similar pretrained Pythia models,

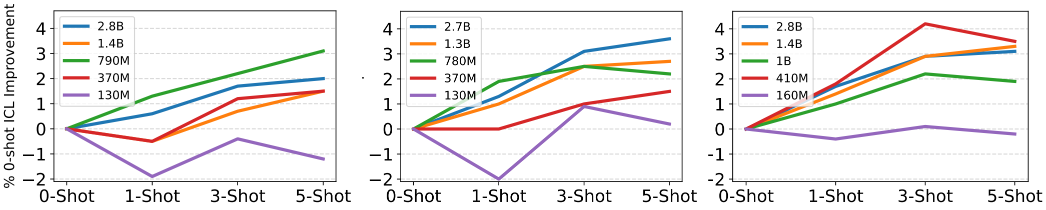

(a) Mamba Pretrained (b) Mamba-2 Pretrained (c) Pythia Pretrained

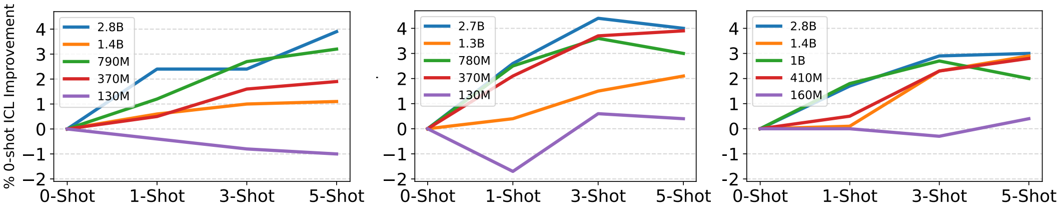

(d) Mamba `ALL LoRA` (e) Mamba-2 `ALL LoRA` (f) Pythia `ALL LoRA`

Figure 3: Instruction tuning narrows the ICL gap between Mamba and Pythia, and creates a gap from Pythia to Mamba-2 models. `ALL LoRA` models were instruction tuned on the OpenHermes (Teknium, 2024) dataset for one epoch. Performance is reported as the average improvement percentage of {1, 3, 5}-shot versus 0-shot over five standard natural language benchmarks.

instruction tuned Mamba and Mamba-2 models are capable of 81.5% and 133% of the AIPSS relative to similarly fine-tuned Pythia models.

In addition to Pythia, we compare instruction tuned Mamba models' ICL abilities to other state-of-the Transformer LLMs of comparable sizes and pretraining token counts: `OpenELM` (Mehta et al., 2024) (sizes `270M`, `450M`, and `1.1B`), `TinyLlama 1.1B` (Zhang et al., 2024), and `OLMo 1.2B` (Groeneveld et al., 2024). We additionally group models by parameter count, to understand ICL as an emergent behavior of fine-tuned Mamba models. Displayed in Appendix F, pretrained SSMs and Transformers of parameter counts 270 million and less display slight or detrimental ICL abilities (i.e., few-shot performance is worse than zero-shot). For models of greater than 450 million parameters, the majority of SSMs and Transformers display positive ICL abilities, with the exception of `Mamba 1.4B`.

Instruction tuning greatly smooths ICL performance across both parameter classes. While instruction tuned SSMs and Transformers of 160 million parameters or fewer continue to display slight or detrimental ICL abilities, all parameters of 270 million and greater show positive ICL abilities. For instruction tuned models of greater than 450 million parameters, all SSMs and Transformers show positive ICL abilities, with `Mamba-2 2.7B` closely matching (or exceeding) the ICL ability of the top performing Transformer LLM per-shot. We note that in terms of an emergent ability (Wei et al., 2022), ICL emerges for instruction tuned Mamba and Mamba-2 SSMs of size 370 million and greater, while no clear trend presents itself for pretrained models.

4 Related Work

Previous work has studied the performance difference for attention-based LLMs under low-precision inference (Dettmers et al., 2022; Dettmers & Zettlemoyer, 2023) and fine-tuning (Dettmers et al., 2024). However, these works only measured divergence using single-shot performance (i.e., zero-shot in (Dettmers et al., 2022; Dettmers & Zettlemoyer, 2023), 5-shot for MMLU and zero-shot otherwise in (Dettmers et al., 2024)). In contrast, we report the difference in model performance as the mean divergence between the full-precision and mixed-precision models, averaged over the accuracy of four different few-shot evaluations. Thus, in contrast to previous work, our inclusion of multiple shots: a) uncovers significant divergence in widely used LLMs even at widely used mixed-precisions (`FP16` and `BF16`), and (b) more rigorously tests mixed-precision training's effect on one of LLMs' most important reasoning abilities (ICL). We are not aware of any previous works which have attempted to understand the performance impact of MPFT on Mamba models.

Recent work has sought to understand the in-context learning (ICL) capabilities of Mamba LLMs when trained from scratch for specific tasks (Park et al., 2024; Lee et al., 2024). Another line of recent work has sought to understand how hybrid Mamba-Transformer models may be directly distilled from Transformer models (Wang et al., 2024b). However, to the best of our knowledge, no existing works have either theoretically explored the effects small input changes (e.g., due to mixed-precision) have on Mamba's recurrent dynamics, empirically explored such effects downstream impact on fine-tuning and inference, or sought to understand the effects of LoRA adaptation on modules within the `MambaBlock`.

Lyapunov exponents have previously been considered (Mikhaeil et al., 2022; Vogt et al., 2022) for classic RNN structures (e.g., vanilla RNNs, LSTMs, GRUs, PLRNNs, etc.), to determine when such models exhibit chaotic dynamics and the impact on the exploding/vanishing gradient phenomena[1].

For S4 (Gu et al., 2022) SSMs, Goel et al. (2022) used Hurwitz matrices to characterize the numerical stability of linear time-invariant (LTI) S4 models. Similarly, Orvieto et al. (2023) used the LTI property to derive the eigenvalue decomposition of S4-like models, providing stability conditions by bounding the corresponding eigenvalues (further discussed in Appendix D). However, such analysis is not applicable to time-varying models, such as Mamba, nor does it characterize the effects of sensitive dependence on initial conditions (e.g., divergence of two ε close inputs). To the best of our knowledge, no previous works have used Lyapunov exponents to explore the effects of mixed-precision on recurrent neural models or Mamba architectures.

As previously noted, recent works (Park et al., 2024; Lee et al., 2024) have studied Mamba's ability to perform ICL by training Mamba models for specific tasks. Such tasks include logistic regression, decision trees, and learning other simple function classes, following the work of Garg et al. (2022). We emphasize that, in this set up, relatively small Mamba models–33 million and 90 million parameters for Lee et al. (2024) and Park et al. (2024), respectively–are trained from scratch for every evaluated task. Indeed, Park et al. (2024) notes that subsequent work is necessary to understand Mamba's ICL capabilities for language modeling using standard natural language benchmarks, as well as for larger model sizes. Thus, our study of both the pretrained and instruction tuned ICL capabilities of Mamba/Mamba-2 LLMs for natural language tasks are complimentary to previous works.

5 Conclusions and Future Directions

Using dynamical systems theory, we've shown that the recurrent dynamics of Mamba SSMs are stable to small input perturbations. We've extensively confirmed this result, showing that Mamba training is significantly more robust to changes introduced during MPFT and PEFT than Transformer-based LLMs across widely-used fine-tuning datasets and benchmarks. Furthermore, by including many more few-shot evaluations in our divergence metric than previous work, our stability studies uncovered that Transformer LLMs are susceptible to large deviation spikes during MPFT alone, as well as when MPFT is combined with PEFT. As MPFT and PEFT are two of the most common LLM fine-tuning frameworks, and as lower precision formats (e.g., `NF4` and `FP8`) become more widely used for fine-tuning, we advocate for more extensive stability analysis (e.g., including several few-shot evaluations when calculating divergence) to expose large deviation spikes.

In order to mitigate large deviation spikes, we've shown that, unlike Transformer LLMs, Mamba models are extremely stable and do not exhibit this phenomena. Furthermore, in addition to stable MPFT and PEFT, we've shown that a core LLM reasoning ability (ICL) of Mamba models significantly improves with instruction tuning; i.e., we've shown that while pretrained Mamba models' ICL capabilities lag behind those of pretrained LLMs on natural language tasks, instruction tuned Mamba models' rival (and surpass, in many Mamba-2 cases) the ICL capabilities of instruction tuned Transformers. Thus, Mamba models are extremely stable learners with the potential to display the ICL capabilities of attention-based models once instruction tuned.

---

[1] We note that this continues a long line of research exploring RNNs sensitivity to initial conditions and their subsequent ability to produce chaotic output (Ribeiro et al., 2020; Laurent & von Brecht, 2017; Bertschinger & Natschläger, 2004; Bertschinger et al., 2004), although previous work did not leverage Lyapunov exponents.

There are several avenues for future work. In particular, adapting Mamba's CUDA kernels to support more aggressive low-precision PEFT methods (Dettmers et al., 2024) would further decrease the hardware needed to train Mamba models, while providing additional speedups and testing the limits of the derived stability results. Furthermore, our theoretical contributions open the door for follow up studies, both in terms of extending our stability results to more general error (and adversarial robustness) results, as well as deriving new SSM-specific LoRA schemes for regularized learning.

Broader Impact Statement

The Mamba models considered are all LLMs, and thus have the same potential positive and negative societal impacts as other LLMs (e.g., hallucinations). Furthermore, fine-tuning is known to possibly erode existing LLM guardrails, and thus our methods may be adapted for this fine-tuning use case (as is the case for all PEFT and MPFT methods). However, our work improves the quality of Mamba models for downstream applications, which may be adapted for all positive LLM applications in society (e.g., personal assistants, task automation, code completion, etc.). Finally, our work decreases the computational constraints required to train and inference Mamba SSMs, which has implications for green ML (e.g., decreased CO2 emissions, positive climate change impact, etc.).

References

Quentin Anthony, Yury Tokpanov, Paolo Glorioso, and Beren Millidge. Blackmamba: Mixture of experts for state-space models. *arXiv preprint arXiv:2402.01771*, 2024.

Yoshua Bengio, Patrice Simard, and Paolo Frasconi. Learning long-term dependencies with gradient descent is difficult. *IEEE transactions on neural networks*, 5(2):157–166, 1994.

Nils Bertschinger and Thomas Natschläger. Real-time computation at the edge of chaos in recurrent neural networks. *Neural computation*, 16(7):1413–1436, 2004.

Nils Bertschinger, Thomas Natschläger, and Robert Legenstein. At the edge of chaos: Real-time computations and self-organized criticality in recurrent neural networks. *Advances in neural information processing systems*, 17, 2004.

Stella Biderman, Hailey Schoelkopf, Quentin Gregory Anthony, Herbie Bradley, Kyle O'Brien, Eric Hallahan, Mohammad Aflah Khan, Shivanshu Purohit, USVSN Sai Prashanth, Edward Raff, et al. Pythia: A suite for analyzing large language models across training and scaling. In *International Conference on Machine Learning (ICML)*, pp. 2397–2430. PMLR, 2023.

Yonatan Bisk, Rowan Zellers, Jianfeng Gao, Yejin Choi, et al. Piqa: Reasoning about physical commonsense in natural language. In *Proceedings of the AAAI conference on artificial intelligence*, volume 34, pp. 7432–7439, 2020.

Tom Brown, Benjamin Mann, Nick Ryder, Melanie Subbiah, Jared D Kaplan, Prafulla Dhariwal, Arvind Neelakantan, Pranav Shyam, Girish Sastry, Amanda Askell, et al. Language models are few-shot learners. *Advances in neural information processing systems*, 33:1877–1901, 2020.

Peter Clark, Isaac Cowhey, Oren Etzioni, Tushar Khot, Ashish Sabharwal, Carissa Schoenick, and Oyvind Tafjord. Think you have solved question answering? try arc, the ai2 reasoning challenge. *arXiv preprint arXiv:1803.05457*, 2018.

Tri Dao and Albert Gu. Transformers are ssms: Generalized models and efficient algorithms through structured state space duality. In *Forty-first International Conference on Machine Learning (ICML)*, 2024.

Tri Dao, Dan Fu, Stefano Ermon, Atri Rudra, and Christopher Ré. Flashattention: Fast and memory-efficient exact attention with io-awareness. *Advances in Neural Information Processing Systems*, 35:16344–16359, 2022.

Tim Dettmers and Luke Zettlemoyer. The case for 4-bit precision: k-bit inference scaling laws. In *International Conference on Machine Learning*, pp. 7750–7774. PMLR, 2023.

Tim Dettmers, Mike Lewis, Younes Belkada, and Luke Zettlemoyer. Gpt3. int8 (): 8-bit matrix multiplication for transformers at scale. *Advances in Neural Information Processing Systems*, 35:30318–30332, 2022.

Tim Dettmers, Artidoro Pagnoni, Ari Holtzman, and Luke Zettlemoyer. Qlora: Efficient finetuning of quantized llms. *Advances in Neural Information Processing Systems*, 36, 2024.

Leo Gao, Jonathan Tow, Baber Abbasi, Stella Biderman, Sid Black, Anthony DiPofi, Charles Foster, Laurence Golding, Jeffrey Hsu, Alain Le Noac'h, Haonan Li, Kyle McDonell, Niklas Muennighoff, Chris Ociepa, Jason Phang, Laria Reynolds, Hailey Schoelkopf, Aviya Skowron, Lintang Sutawika, Eric Tang, Anish Thite, Ben Wang, Kevin Wang, and Andy Zou. A framework for few-shot language model evaluation, 12 2023. URL `https://zenodo.org/records/10256836`.

Shivam Garg, Dimitris Tsipras, Percy S Liang, and Gregory Valiant. What can transformers learn in-context? a case study of simple function classes. *Advances in Neural Information Processing Systems (NeurIPS)*, 35: 30583–30598, 2022.

Karan Goel, Albert Gu, Chris Donahue, and Christopher Ré. It's raw! audio generation with state-space models. In *International Conference on Machine Learning*, pp. 7616–7633. PMLR, 2022.

Dirk Groeneveld, Iz Beltagy, Pete Walsh, Akshita Bhagia, Rodney Kinney, Oyvind Tafjord, Ananya Harsh Jha, Hamish Ivison, Ian Magnusson, Yizhong Wang, et al. Olmo: Accelerating the science of language models. *arXiv preprint arXiv:2402.00838*, 2024.

Albert Gu and Tri Dao. Mamba: Linear-time sequence modeling with selective state spaces. In *First Conference on Language Modeling*, 2024a. URL `https://openreview.net/forum?id=tEYskw1VY2`.

Albert Gu and Tri Dao. *Mamba Precision Guidance*. "`https://github.com/state-spaces/mamba#precision`", 2024b. "Accessed: 2024-04-25".

Albert Gu, Karan Goel, and Christopher Re. Efficiently modeling long sequences with structured state spaces. In *International Conference on Learning Representations (ICLR)*, 2022.

Dan Hendrycks, Collin Burns, Steven Basart, Andy Zou, Mantas Mazeika, Dawn Song, and Jacob Steinhardt. Measuring massive multitask language understanding. In *International Conference on Learning Representations*, 2020.

Edward J Hu, Yelong Shen, Phillip Wallis, Zeyuan Allen-Zhu, Yuanzhi Li, Shean Wang, Lu Wang, and Weizhu Chen. Lora: Low-rank adaptation of large language models. *arXiv preprint arXiv:2106.09685*, 2021.

Huggingface. *Mamba PEFT*. "`https://huggingface.co/docs/transformers/en/model_doc/mamba#peft-finetuning`", 2024. "Accessed: 2024-04-25".

Tanguy Laffargue, Khanh-Dang Nguyen Thu Lam, Jorge Kurchan, and Julien Tailleur. Large deviations of lyapunov exponents. *Journal of Physics A: Mathematical and Theoretical*, 46(25):254002, 2013.

Thomas Laurent and James von Brecht. A recurrent neural network without chaos. In *Proceedings of the 11th International Conference on Learning Representations (ICLR)*, 2017.

Ivan Lee, Nan Jiang, and Taylor Berg-Kirkpatrick. Is attention required for icl? exploring the relationship between model architecture and in-context learning ability. In *The Twelfth International Conference on Learning Representations (ICLR)*, 2024.

Kai Li and Guo Chen. Spmamba: State-space model is all you need in speech separation. *arXiv preprint arXiv:2404.02063*, 2024.

Lincan Li, Hanchen Wang, Wenjie Zhang, and Adelle Coster. Stg-mamba: Spatial-temporal graph learning via selective state space model. *arXiv preprint arXiv:2403.12418*, 2024.

Opher Lieber, Barak Lenz, Hofit Bata, Gal Cohen, Jhonathan Osin, Itay Dalmedigos, Erez Safahi, Shaked Meirom, Yonatan Belinkov, Shai Shalev-Shwartz, et al. Jamba: A hybrid transformer-mamba language model. *arXiv preprint arXiv:2403.19887*, 2024.

Yue Liu, Yunjie Tian, Yuzhong Zhao, Hongtian Yu, Lingxi Xie, Yaowei Wang, Qixiang Ye, and Yunfan Liu. Vmamba: Visual state space model. *arXiv preprint arXiv:2401.10166*, 2024.

Sachin Mehta, Mohammad Hossein Sekhavat, Qingqing Cao, Maxwell Horton, Yanzi Jin, Chenfan Sun, Iman Mirzadeh, Mahyar Najibi, Dmitry Belenko, Peter Zatloukal, et al. Openelm: An efficient language model family with open-source training and inference framework. *arXiv preprint arXiv:2404.14619*, 2024.

Jonas Mikhaeil, Zahra Monfared, and Daniel Durstewitz. On the difficulty of learning chaotic dynamics with rnns. *Advances in Neural Information Processing Systems*, 35:11297–11312, 2022.

Antonio Orvieto, Samuel L Smith, Albert Gu, Anushan Fernando, Caglar Gulcehre, Razvan Pascanu, and Soham De. Resurrecting recurrent neural networks for long sequences. In *International Conference on Machine Learning*, pp. 26670–26698. PMLR, 2023.

Jongho Park, Jaeseung Park, Zheyang Xiong, Nayoung Lee, Jaewoong Cho, Samet Oymak, Kangwook Lee, and Dimitris Papailiopoulos. Can mamba learn how to learn? a comparative study on in-context learning tasks. *International Conference on Machine Learning (ICML)*, 2024.

Razvan Pascanu, Tomas Mikolov, and Yoshua Bengio. On the difficulty of training recurrent neural networks. In *Proceedings of the 30th International Conference on International Conference on Machine Learning-Volume 28*, pp. III–1310, 2013.

Changsheng Quan and Xiaofei Li. Multichannel long-term streaming neural speech enhancement for static and moving speakers. *arXiv preprint arXiv:2403.07675*, 2024.

Antônio H Ribeiro, Koen Tiels, Luis A Aguirre, and Thomas Schön. Beyond exploding and vanishing gradients: analysing rnn training using attractors and smoothness. In *International conference on artificial intelligence and statistics (AISTATS)*, pp. 2370–2380. PMLR, 2020.

Keisuke Sakaguchi, Ronan Le Bras, Chandra Bhagavatula, and Yejin Choi. Winogrande: An adversarial winograd schema challenge at scale. *Communications of the ACM*, 64(9):99–106, 2021.

Hiroki Sayama. *Introduction to the modeling and analysis of complex systems*. Open SUNY Textbooks, 2015.

Rohan Taori, Ishaan Gulrajani, Tianyi Zhang, Yann Dubois, Xuechen Li, Carlos Guestrin, Percy Liang, and Tatsunori B. Hashimoto. Stanford alpaca: An instruction-following llama model. `https://github.com/tatsu-lab/stanford_alpaca`, 2023.

Teknium. *Openhermes*. "`https://huggingface.co/datasets/teknium/openhermes`", 2024. "Accessed: 2024-04-25".

Lewis Tunstall, Edward Beeching, Nathan Lambert, Nazneen Rajani, Kashif Rasul, Younes Belkada, Shengyi Huang, Leandro von Werra, Clémentine Fourrier, Nathan Habib, et al. Zephyr: Direct distillation of lm alignment. *arXiv preprint arXiv:2310.16944*, 2023.

Ryan Vogt, Maximilian Puelma Touzel, Eli Shlizerman, and Guillaume Lajoie. On lyapunov exponents for rnns: Understanding information propagation using dynamical systems tools. *Frontiers in Applied Mathematics and Statistics*, 8:818799, 2022.

Chloe Wang, Oleksii Tsepa, Jun Ma, and Bo Wang. Graph-mamba: Towards long-range graph sequence modeling with selective state spaces. *arXiv preprint arXiv:2402.00789*, 2024a.

Junxiong Wang, Daniele Paliotta, Avner May, Alexander M Rush, and Tri Dao. The mamba in the llama: Distilling and accelerating hybrid models. In *Workshop on Efficient Systems for Foundation Models II@ ICML2024*, 2024b.

Jason Wei, Yi Tay, Rishi Bommasani, Colin Raffel, Barret Zoph, Sebastian Borgeaud, Dani Yogatama, Maarten Bosma, Denny Zhou, Donald Metzler, et al. Emergent abilities of large language models. *Transactions on Machine Learning Research*, 2022.

Jianhao Xie, Ruofan Liao, Ziang Zhang, Sida Yi, Yuesheng Zhu, and Guibo Luo. Promamba: Prompt-mamba for polyp segmentation. *arXiv preprint arXiv:2403.13660*, 2024.

Sang Michael Xie, Aditi Raghunathan, Percy Liang, and Tengyu Ma. An explanation of in-context learning as implicit bayesian inference. In *International Conference on Learning Representations (ICLR)*, 2021.

Rowan Zellers, Ari Holtzman, Yonatan Bisk, Ali Farhadi, and Yejin Choi. Hellaswag: Can a machine really finish your sentence? In *Proceedings of the 57th Annual Meeting of the Association for Computational Linguistics*, pp. 4791–4800, 2019.

Peiyuan Zhang, Guangtao Zeng, Tianduo Wang, and Wei Lu. Tinyllama: An open-source small language model. *arXiv preprint arXiv:2401.02385*, 2024.

Chunting Zhou, Pengfei Liu, Puxin Xu, Srinivasan Iyer, Jiao Sun, Yuning Mao, Xuezhe Ma, Avia Efrat, Ping Yu, Lili Yu, et al. Lima: Less is more for alignment. *Advances in Neural Information Processing Systems*, 36, 2024.

A Mamba stable dynamics proof

Recall the state-space parameters and equations for the `MambaBlock`; $\mathbf{A}, \mathbf{B}_t, \mathbf{C}_t, \mathbf{\Delta}_t \in \mathbb{R}^{d \times d}$ for $t \in \{1, \dots, T\} = [T]$. Given an input sequence $\mathbf{u}_1, \dots, \mathbf{u}_T \in \mathbb{R}^d$, the following linear mapping through latent states $\boldsymbol{x}_1, \dots, \boldsymbol{x}_T \in \mathbb{R}^d$ is used to produce the output $\mathbf{y}_1, \dots, \mathbf{y}_T \in \mathbb{R}^d$:

$$\begin{aligned} \boldsymbol{x}_t &= \bar{\mathbf{A}}_t \boldsymbol{x}_{t-1} + \bar{\mathbf{B}}_t \mathbf{u}_t \\ \mathbf{y}_t &= \mathbf{C}_t \boldsymbol{x}_t, \end{aligned} \tag{8}$$

where $\bar{\mathbf{\Delta}}_t = \texttt{softplus}(\texttt{Linear}(\mathbf{\Delta}_t)) \in \mathbb{R}_{\geqslant 0}{}^{d \times d}$, $\bar{\mathbf{A}}_t = \exp(\bar{\mathbf{\Delta}}_t \mathbf{A})$, $\bar{\mathbf{B}}_t = \mathbf{A}^{-1}(\bar{\mathbf{A}} - \mathbf{I})\mathbf{B}_t$, and $\mathbb{R}_{\geqslant 0}$ is the set of non-negative real numbers. In practice, $\mathbf{A}, \mathbf{B}_t, \mathbf{C}_t$ and $\mathbf{\Delta}_t$ are diagonal matrices.

Furthermore, recall the following definitions:

$$\boldsymbol{x}_t = F_\theta(\boldsymbol{x}_{t-1}, \mathbf{u}_t)$$

where θ denotes the aforementioned time-varying parameters. For input sequence $\mathbf{u}_t, \dots, \mathbf{u}_T$ and initial latent state value $\boldsymbol{x}_0$, we thus write

$$\boldsymbol{x}_T = F_\theta(F_\theta(\dots F_\theta(\boldsymbol{x}_0, \mathbf{u}_1))) \coloneqq F_\theta^{T-1}(\boldsymbol{x}_0, \mathbf{u}_1).$$

We first prove that, given two scalar ε-close inputs to a `MambaBlock`, their deviations do not grow exponentially as the number of recurrences increases (Lemma 1). The main result in the paper is subsequently proved.

Lemma 1. *For input* $(\boldsymbol{x}_0, \mathbf{u}_1)$ *to a* `MambaBlock`*, small changes* $(\boldsymbol{x}_0 + \varepsilon, \mathbf{u}_1 + \varepsilon)$ *produce deviations which are exponentially non-increasing over discrete-time. That is,* $\max |F_\theta^N(\boldsymbol{x}_0, \mathbf{u}_1) - F_\theta^N(\boldsymbol{x}_0 + \varepsilon, \mathbf{u}_1 + \varepsilon)| \in \mathcal{O}(\varepsilon \exp(N\zeta))$*, for some scalar* $\zeta \leqslant 0$.

Proof. Firstly, we note that within the `MambaBlock`, $\mathbf{A}$ is stored in log-space followed by a negative exponentiation prior to use. Thus, $\mathbf{A} \in \mathbb{R}_{\leqslant 0}{}^{d \times d}$, where $\mathbb{R}_{\leqslant 0}$ is the set of non-positive real numbers.

Recall that for the maximum deviation, we have:

$$\max |F_\theta^N(\boldsymbol{x}_0, \mathbf{u}_1) - F_\theta^N(\boldsymbol{x}_0 + \varepsilon, \mathbf{u}_1 + \varepsilon)| \in \mathcal{O}(\varepsilon \exp(N\lambda_{\texttt{max}})).$$

where the maximal Lyapunov exponent $\lambda_{\texttt{max}}$ is defined as:

$$\lambda_{\texttt{max}} \coloneqq \lim_{T\to\infty} \frac{1}{T} \log \left\| \prod_{t=0}^{T} \frac{\partial \boldsymbol{x}_t}{\partial \boldsymbol{x}_{t-1}} \right\|_2 ,$$

and $\|\|_2$ denotes the spectral norm for matrices.

Thus, to complete the proof, it suffices to show that $\lambda_{\texttt{max}} \leqslant 0$. Recall that $\mathbf{A}$ and $\bar{\boldsymbol{\Delta}}_t$ are diagonal. From Equation 8, we thus have

$$\begin{aligned}\lambda_{\texttt{max}} &= \lim_{T\to\infty} \frac{1}{T} \log \left\| \prod_{t=0}^{T} \frac{\partial \boldsymbol{x}_t}{\partial \boldsymbol{x}_{t-1}} \right\|_2 \\ &= \lim_{T\to\infty} \frac{1}{T} \log \left\| \prod_{t=0}^{T} \exp\left(\bar{\boldsymbol{\Delta}}_t \mathbf{A}\right) \right\|_2 \\ &= \lim_{T\to\infty} \frac{1}{T} \log \left\| \exp \sum_{t=0}^{T} (\bar{\boldsymbol{\Delta}}_t \mathbf{A}) \right\|_2\end{aligned}$$

Let i be the dimension which corresponds to the output of the spectral norm, i.e., $i = \operatorname{argmax}_{j=1,\ldots,d}\{\exp \sum_{t=0}^{T} (\bar{\boldsymbol{\Delta}}_t[j,j]\mathbf{A}[j,j])\}$. We thus have

$$\begin{aligned}\lambda_{\texttt{max}} &= \lim_{T\to\infty} \frac{1}{T} \log \left\| \exp \sum_{t=0}^{T} (\bar{\boldsymbol{\Delta}}_t \mathbf{A}) \right\|_2 \\ &= \lim_{T\to\infty} \frac{1}{T} \log \exp \sum_{t=0}^{T} (\bar{\boldsymbol{\Delta}}_t[i,i]\mathbf{A}[i,i]) \\ &= \mathbf{A}[i,i] \lim_{T\to\infty} \frac{1}{T} \sum_{t=0}^{T} \bar{\boldsymbol{\Delta}}_t[i,i]\end{aligned}$$

$\mathbf{A}[i,i]$ is non-positive and $\lim_{T\to\infty} \frac{1}{T} \sum_{t=0}^{T} \bar{\boldsymbol{\Delta}}_t[i,i] \geqslant 0$, since $\bar{\boldsymbol{\Delta}}_t[i,i] \in \mathbb{R}_{\geqslant 0}\ \forall t$. Thus, $\lambda_{\texttt{max}} \leqslant 0$. ☐

Theorem 4. *Let $(\boldsymbol{x}_{t-1}, \mathbf{u}_t)$ be the latent state and input at an arbitrary time $t \in [1, T]$ within a `MambaBlock`. Then small changes $(\boldsymbol{x}_{t-1} + \varepsilon, \mathbf{u}_t + \varepsilon)$ produce deviations which are exponentially decreasing over discrete-time, i.e., $\max |F_\theta^N(\boldsymbol{x}_0, \mathbf{u}_1) - F_\theta^N(\boldsymbol{x}_0 + \varepsilon, \mathbf{u}_1 + \varepsilon)| \in \mathcal{O}(\varepsilon \exp(N\zeta))$, for some scalar $\zeta \leqslant 0$.*

Proof. Let $\tau(t)$ be a function that maps time values such that $\tau(t) \in [1, T-t]$ and $\tau(t) = 1, \tau(t+1) = 2, \ldots, \tau(t+T) = T-t$. Then $\mathbf{B}_{\tau(t)}, \mathbf{C}_{\tau(t)}, \boldsymbol{\Delta}_{\tau(t)}$ define a new `MambaBlock` with inputs $\mathbf{u}_{\tau(t)}, \ldots, \mathbf{u}_{\tau(t+T)}$ and subsequent recurrent states $\boldsymbol{x}_{\tau(t)}, \ldots, \boldsymbol{x}_{\tau(t+T)}$. Applying Lemma 1 to this `MambaBlock` with $(\boldsymbol{x}_{\tau(t)-1}, \mathbf{u}_{\tau(t)})$ completes the proof. ☐

B Mamba stable outputs proof

Theorem 5. *Assume $(\boldsymbol{x}_{t-1} + \varepsilon, \mathbf{u}_t + \varepsilon)$ produce deviations which are exponentially non-increasing over discrete-time. Then small changes to the output $\mathbf{y}_t$ are also exponentially non-increasing over discrete time.*

Proof. Recall that $\boldsymbol{x}_T = F_\theta^T(\boldsymbol{x}_0, \mathbf{u}_1)$. Furthermore, recall from Equations 1 and 2, $\mathbf{y}_t = \mathbf{C}_t \boldsymbol{x}_t$, where $\mathbf{C}_t$ is diagonal.

Let

$$\mathbf{y}_T = G_\theta^T(\boldsymbol{x}_0, \mathbf{u}_1) = \mathbf{C}_T \boldsymbol{x}_T = \mathbf{C}_T F_\theta^T(\boldsymbol{x}_0, \mathbf{u}_1).$$

Consider ε-close inputs $(\boldsymbol{x}_{t-1}, \mathbf{u}_t)$ and $(\boldsymbol{x}_{t-1} + \varepsilon, \mathbf{u}_t + \varepsilon)$, and their respective outputs $\mathbf{y}_t$ and $\mathbf{y}'_t$. Assume $(\boldsymbol{x}_{t-1} + \varepsilon, \mathbf{u}_t + \varepsilon)$ produce deviations which are exponentially non-increasing over discrete-time. That is, $\max |F^N_\theta(\boldsymbol{x}_{t-1}, \mathbf{u}_t) - F^N_\theta(\boldsymbol{x}_{t-1} + \varepsilon, \mathbf{u}_t + \varepsilon)| \in \mathcal{O}(\varepsilon \exp(N\zeta))$, for some scalar $\zeta \leqslant 0$.

We thus have

$$\begin{aligned}\max |\mathbf{y}_t - \mathbf{y}'_t| &= \max |G^N_\theta(\boldsymbol{x}_{t-1}, \mathbf{u}_t) - G^N_\theta(\boldsymbol{x}_{t-1} + \varepsilon, \mathbf{u}_t + \varepsilon)| \\ &= \max |\mathbf{C}_N F^N_\theta(\boldsymbol{x}_{t-1}, \mathbf{u}_t) - \mathbf{C}_N F^N_\theta(\boldsymbol{x}_{t-1} + \varepsilon, \mathbf{u}_t + \varepsilon)| \\ &\propto \max |F^N_\theta(\boldsymbol{x}_{t-1}, \mathbf{u}_t) - F^N_\theta(\boldsymbol{x}_{t-1} + \varepsilon, \mathbf{u}_t + \varepsilon)|,\end{aligned}$$

where proportionality follows due to the diagonality of $\mathbf{C}_N$ and the vector-absolute value. Thus,

$$\max |G^N_\theta(\boldsymbol{x}_{t-1}, \mathbf{u}_t) - G^N_\theta(\boldsymbol{x}_{t-1} + \varepsilon, \mathbf{u}_t + \varepsilon)| \in \mathcal{O}(\varepsilon \exp(N\zeta))$$

□

C Proof of weight-tying using LoRA in the `MambaBlock`

Due to the low-level nature of Mamba's prefix scan optimizations (discussed in Section 2), standard use of LoRA adapters is made difficult within Mamba's SSM-layer. E.g., while B_t, C_t and Δ_t are conceptually `PyTorch` linear layers, their bundling in a contiguous memory block and careful manipulation makes appending a LoRA adapter on any of these individual matrices non-trivial (particularly, while respecting the highly specialized layout of each LoRA adapters targeted layer). However, we note that the overall design of the `MambaBlock`'s hardware optimizations may be leveraged to both efficiently learn the parameter-space for the majority of time-varying parameters (thus achieving PEFT) and regularize parameters during training (thus improving fine-tuning generalization).

Theorem 6. *Consider the weight matrix $\mathbf{W}$ of a `MambaBlock` from Equation 4. Targeting $\mathbf{W}$ for LoRA during fine-tuning ties adaptation weights across $\mathbf{B}_t, \mathbf{C}_t$ and $\boldsymbol{\Delta}_t$.*

Proof. Let r be the specified LoRA dimension. Targeting this matrix for LoRA results in the adapter

$$\begin{aligned}\tilde{\mathbf{W}} =& \mathbf{W} + \mathbf{W}' \\ =& \mathbf{W} + \mathbf{U}\mathbf{V},\end{aligned}$$

where $\mathbf{U} \in \mathbb{R}^{n \times r}$, $\mathbf{V} \in \mathbb{R}^{r \times 3d}$, and $\mathbf{W}$ is frozen during fine-tuning. Thus, for index $[i, j]$,

$$\mathbf{W}'[i, j] = \sum_{k=0}^{r-1} \mathbf{U}[i, k]\mathbf{V}[k, j].$$

Recall the form of $\mathbf{W}$:

$$\mathbf{W}[t-1, : d] = \mathtt{diag}(\boldsymbol{\Delta}_t), \mathbf{W}[t-1, d : 2d] = \mathtt{diag}(\mathbf{B}_t), \mathbf{W}[t-1, 2d : 3d] = \mathtt{diag}(\mathbf{C}_t),$$

where $\mathbf{W}[0, : d] = \mathtt{diag}(\boldsymbol{\Delta}_1), \mathbf{W}[n-1, d : 2d] = \mathtt{diag}(\mathbf{B}_T)$, and so on. For index $[t-1, j]$, we thus have

$$\begin{aligned}\tilde{\mathbf{W}}[t-1, j] =& \mathbf{W}[t-1, j] + \mathbf{W}'[t-1, j] \\ =& \mathbf{W}[t-1, j] + \sum_{k=0}^{r-1} \mathbf{U}[t-1, k]\mathbf{V}[k, j].\end{aligned}$$

Thus, the weights $\mathbf{U}[t-1, :]$ are tied for any parameter $\tilde{\mathbf{W}}[t-1, j], j \in \{1, \ldots, 3d\}$, which are used to adapt parameters $\boldsymbol{\Delta}_1, \mathbf{B}_t$, and $\mathbf{C}_t$.

□

D Previous SSM stability results

Previous SSM stability results (Goel et al., 2022; Orvieto et al., 2023) consider the following *linear time-invariant* (LTI) equations used in S4 models,

$$\boldsymbol{x}_t = \bar{\mathbf{A}}\boldsymbol{x}_{t-1} + \bar{\mathbf{B}}\mathbf{u}_t \tag{9}$$

$$\mathbf{y}_t = \mathbf{C}\boldsymbol{x}_t., \tag{10}$$

which can be unrolled to produce

$$\boldsymbol{x}_k = \sum_{j=0}^{k} \bar{\mathbf{A}}^j \bar{\mathbf{B}}\mathbf{u}_j. \tag{11}$$

By eigendecomposition,

$$\bar{\mathbf{A}}^j = (\mathbf{P}\mathbf{\Lambda}\mathbf{P}^{-1})^j = \mathbf{P}\mathbf{\Lambda}^j\mathbf{P}^{-1}.$$

In (Orvieto et al., 2023), the derived sufficient condition for stability is thus $|\alpha_i| \leqslant 1$, for $\mathbf{\Lambda} = \texttt{diag}([\alpha_0, \alpha_1, \ldots, \alpha_d])$. Relatedly, in (Goel et al., 2022), stability is enforced by constraining $\mathbf{\Lambda}$ to be Hurwitz, in which case the real part of each diagonal entry α_i is negative, i.e., $\mathrm{Re}(\alpha_i) < 0$, for $\mathbf{\Lambda} = \texttt{diag}([\alpha_0, \alpha_1, \ldots, \alpha_d])$.

Both results critically rely on the LTI property of Equations 9 and 10 to derive Equation 11. However, Mamba's state-space equations are *linear time-varying* (LTV), and thus Equation 11 does not hold. Thus, previous SSM stability results do not directly apply to Mamba models.

E Experimental Details

All model checkpoints were evaluated on all benchmarks and few-shot settings using the LM evaluation harness from Eleuther AI (Gao et al., 2023), version `0.4.2`. Pythia and Mamba `Huggingface` checkpoints were used for all inference and fine-tuning experiments, e.g., `EleutherAI/pythia-160m` and `state-spaces/mamba-130m-hf` for the smallest respective models. All fine-tuning experiments were run using package versions `Transformers 4.40.0.dev0`, `Accelerate 0.28.0`, `TRL 0.8.1`, `PyTorch 2.2.1+cu121`, and `PEFT 0.10.0`. All Mamba-2 models were run using `mamba-ssm v2.2.2` using `Huggingface` checkpoints, e.g., `state-spaces/mamba-130m` for the smallest model.

For MPFT, `Flash Attention 2.0` (Dao et al., 2022) via `flash_attn 2.5.7` was used for Pythia models. For `FP16` and `BF16` inference results, Flash Attention 2.0 was used for both Pythia and OLMo models. For OLMo results, the 336B-token checkpoint was used by specifying `revision=step80000-tokens336B`.

All Alpaca and OpenHermes fine-tuning experiments used the following training recipe (adapted from (Tunstall et al., 2023)): `AdamW_torch` optimizer, `cosine annealing` schedule, no gradient accumulation, maximum norm of 1.0 for gradient clipping, and no warmup steps. Training epochs used for all Alpaca and OpenHermes experiments were three and one, respectively. For both Pythia and Mamba models, the learning rate and LoRA dimension r were scaled to improve performance of smaller models (per-model values listed in Table 1).

For `SLL LoRA`, targeted Mamba layers were `{x_proj, embeddings, in_proj, out_proj}`; `x_proj` is the large `MambaBlock` memory buffer which, when targeted by LoRA, regularizes the majority of SSM parameters during fine-tuning through weight tying (Theorem 3). Pythia targeted `SLL LoRA` layers were `{dense, embed_in, query_key_value, dense_h_to_4h,dense_4h_to_h}`, chosen to balance performance across model sizes.

All experiments were run using a single-GPU Nvidia A10G (24 GB total memory). For Pythia, Mamba, and Mamba-2 `ALL LoRA` experiments in Figure 3, all models followed the same training and PEFT recipes, save for Mamba-2 `2.7B` which required a LoRA r dimension of 64 to fit in A10G memory.

Table 1: Learning rate and LoRA dimension r values

Mamba size	Mamba-2 size	Pythia size	learning rate	Mamba/Pythia LoRA r	Mamba-2 LoRA r
`130M`	`130M`	`160M`	1.0e-5	8	8
`370M`	`370M`	`410M`	5.0e-5	16	16
`790M`	`780M`	`1B`	1.0e-6	32	32
`1.4B`	`1.3B`	`1.4B`	5.0e-6	64	64
`2.8B`	`2.7B`	`2.8B`	5.0e-7	128	64

The Alpaca dataset is freely available for download at `https://huggingface.co/datasets/tatsu-lab/alpaca` under open-source license `CC-by-NC 4.0`. The OpenHermes dataset is freely available for download at `https://huggingface.co/datasets/teknium/OpenHermes-2.5` under open-source license `MIT, Apache 2.0, CC`.

Table 2: **Pretrained model performance**. Model checkpoints were evaluated on all benchmarks and few-shot settings using the LM evaluation harness from Eleuther AI (Gao et al., 2023). LAMBADA zero-shot is more effective for the model sizes considered (further discussed in (Xie et al., 2021; Brown et al., 2020)) and thus excluded from few-shot performance averages. Highlighted in bold is the top-performing few-shot learner per benchmark and model grouping.

Model	N-shot	LAMBADA ppl ↓	LAMBADA acc ↑	HellaSwag acc ↑	PIQA acc ↑	Arc-E acc ↑	Arc-C acc ↑	WinoGrande acc ↑	0-shot incr. Mean % ↑
Mamba 130M	0	**16.0**	**44.3**	35.2	64.7	48.0	24.3	52.6	–
	1	19.3	38.2	35.1	64.6	47.0	23.5	50.8	-1.9
	3	23.1	35.2	35.0	65.1	49.1	24.0	51.0	-0.4
	5	24.4	36.2	34.9	64.9	49.1	23.7	50.0	-1.2
Mamba-2 130M	0	16.8	43.9	35.3	64.9	47.4	24.2	52.6	–
	1	20.6	37.9	34.9	64.1	46.9	23.1	51.3	-2.0
	3	24.3	35.1	34.9	64.4	**49.0**	24.7	**52.9**	**0.9**
	5	26.5	34.9	34.6	64.4	48.6	**24.8**	51.7	0.2
Pythia 160M	0	38.2	32.7	30.2	61.8	43.4	23.8	51.0	–
	1	47.2	28.2	30.6	62.2	43.4	23.7	49.3	-0.4
	3	63.7	24.7	30.5	61.9	44.8	22.9	51.3	0.1
	5	66.3	25.3	30.4	62.6	43.4	23.1	50.8	-0.2
Mamba 370M	0	8.1	55.6	46.5	69.5	54.9	27.8	55.3	–
	1	9.7	49.8	45.9	69.3	57.4	26.5	54.7	-0.5
	3	10.9	48.4	46.2	69.5	58.8	28.4	53.8	1.2
	5	11.4	48.6	46.2	69.4	58.3	28.0	**55.9**	1.5
Mamba-2 370M	0	**8.0**	**55.9**	**46.9**	**70.5**	54.8	26.7	55.4	–
	1	9.8	50.3	46.4	**70.5**	56.5	26.8	54.2	0.0
	3	11.3	48.5	46.6	70.2	**59.0**	26.9	54.3	1.0
	5	12.5	46.6	46.7	70.3	58.5	28.2	53.3	1.5
Pythia 410M	0	10.8	51.5	40.6	66.9	52.0	24.1	53.4	–
	1	12.3	47.1	40.5	68.0	53.8	25.6	52.4	1.8
	3	14.4	43.2	40.9	67.9	55.1	26.9	54.0	**4.2**
	5	14.6	44.1	40.8	68.1	54.6	26.6	53.4	3.5
Mamba 790M	0	6.0	61.4	**55.1**	72.3	61.2	29.5	55.9	–
	1	7.1	55.9	54.5	72.4	63.0	30.2	56.9	1.3
	3	8.1	54.5	54.2	72.3	63.5	31.4	57.1	2.2
	5	8.8	52.9	54.6	**72.6**	**64.4**	31.9	57.2	**3.1**
Mamba-2 780M	0	**5.9**	**61.7**	54.9	72.0	61.0	28.5	**60.2**	–
	1	7.1	55.5	54.7	72.4	62.3	32.1	57.1	1.9
	3	8.6	53.3	54.7	72.5	62.8	**32.3**	57.8	2.5
	5	9.9	51.4	55.2	72.1	62.8	32.2	56.8	2.2
Pythia 1B	0	7.9	56.3	47.2	70.7	57.0	27.0	53.4	–
	1	8.0	51.8	47.3	70.7	57.1	28.2	53.4	1.0
	3	10.5	48.2	47.5	71.2	59.2	28.0	54.3	2.2
	5	10.9	48.4	47.3	71.4	58.7	28.4	53.1	1.9
Mamba 1.4B	0	**5.0**	64.9	59.2	74.1	65.5	32.9	61.3	–
	1	5.8	60.6	58.2	**74.7**	64.5	33.0	60.9	-0.5
	3	6.6	58.9	58.9	73.6	66.1	34.5	60.9	0.7
	5	7.0	58.3	59.0	74.1	66.4	35.5	60.4	1.5
Mamba-2 1.3B	0	**5.0**	**65.6**	60.0	73.2	64.2	33.1	61.1	–
	1	6.0	60.1	59.4	73.1	65.6	35.3	59.4	1.0
	3	6.7	58.6	60.1	73.4	**66.5**	35.4	**61.9**	2.5
	5	7.0	58.6	**60.2**	73.7	66.5	**35.9**	61.4	2.7
Pythia 1.4B	0	6.1	61.7	52.1	70.9	60.5	28.5	57.4	–
	1	7.0	56.3	52.1	71.4	62.0	29.5	57.5	1.4
	3	7.9	54.4	52.6	70.9	63.9	31.1	56.8	2.9
	5	8.0	54.4	52.8	71.0	63.2	31.3	57.8	**3.3**
Mamba 2.8B	0	4.2	69.1	66.1	75.2	69.6	36.4	63.3	–
	1	5.0	63.7	65.6	75.6	69.9	37.1	63.9	0.6
	3	5.5	62.8	65.5	75.3	70.8	38.1	65.1	1.7
	5	5.7	62.5	66.1	76.1	70.9	38.1	64.6	2.0
Mamba-2 2.7B	0	**4.1**	**69.6**	66.6	**76.4**	69.5	36.3	63.9	–
	1	4.8	65.1	65.9	75.1	70.0	38.6	65.1	1.3
	3	5.3	63.9	66.8	75.2	**71.9**	41.0	64.1	3.1
	5	5.7	62.3	**67.1**	75.3	70.7	**41.2**	**65.9**	**3.6**
	0	5.0	64.7	59.3	73.9	64.2	32.9	59.8	–

Table 3: **Instruction tuned model performance**. Model checkpoints were evaluated on all benchmarks and few-shot settings using the LM evaluation harness from Eleuther AI (Gao et al., 2023). LAMBADA zero-shot is more effective for the model sizes considered (further discussed in (Xie et al., 2021; Brown et al., 2020)) and thus excluded from few-shot performance averages. Highlighted in bold is the top-performing few-shot learner per benchmark and model grouping.

Model	N-shot	LAMBADA ppl ↓	LAMBADA acc ↑	HellaSwag acc ↑	PIQA acc ↑	Arc-E acc ↑	Arc-C acc ↑	WinoGrande acc ↑	0-shot incr. Mean % ↑
Mamba 130M	0	**12.9**	**46.5**	**35.1**	64.2	48.7	**25.5**	51.7	–
	1	17.8	38.1	35.0	64.2	48.6	24.9	**52.2**	-0.4
	3	22.3	35.3	34.8	64.2	**50.2**	24.5	50.6	-0.8
	5	23.6	35.9	34.7	64.7	49.8	24.6	50.2	-0.9
Mamba-2 130M	0	15.2	44.5	**35.1**	64.5	47.2	24.7	**52.2**	–
	1	21.9	36.1	34.5	64.3	46.8	24.0	50.8	-1.7
	3	26.9	33.3	34.7	**65.1**	48.5	25.2	51.5	**0.6**
	5	29.0	33.8	34.5	64.8	48.7	25.1	51.3	0.4
Pythia 160M	0	30.2	36.1	30.0	62.2	44.7	23.6	50.3	–
	1	44.5	29.1	30.4	62.0	44.0	23.6	50.5	-0.0
	3	66.7	25.5	30.3	62.8	45.2	22.8	49.8	-0.3
	5	70.4	25.3	30.5	62.9	44.1	23.4	50.8	0.3
Mamba 370M	0	7.2	**56.0**	46.3	69.2	55.3	27.7	**56.0**	–
	1	9.3	49.9	45.7	68.7	57.1	28.3	55.4	0.5
	3	10.4	49.4	45.7	68.9	58.7	**29.7**	54.1	1.6
	5	11.0	48.3	45.7	70.1	59.3	29.1	54.5	1.9
Mamba-2 370M	0	**7.6**	54.7	**46.8**	69.3	52.2	27.0	**56.0**	–
	1	9.9	48.3	46.0	69.6	55.7	28.8	55.2	2.1
	3	11.8	46.3	46.3	70.1	59.0	29.1	54.5	3.6
	5	12.6	45.5	46.3	**70.8**	**59.6**	29.5	53.0	**3.8**
Pythia 410M	0	13.3	46.4	40.9	67.4	52.7	25.4	53.4	–
	1	17.2	40.4	40.5	68.4	53.6	25.7	53.0	0.5
	3	21.1	37.4	40.9	67.7	55.7	27.1	52.6	2.3
	5	21.5	38.2	40.7	67.8	55.7	27.3	53.8	2.8
Mamba 790M	0	5.2	62.8	55.6	72.8	62.4	30.6	56.2	–
	1	6.3	56.6	54.9	72.7	64.6	31.7	56.3	1.2
	3	7.0	55.6	54.7	72.4	**65.3**	33.2	57.5	2.7
	5	7.5	54.6	54.9	72.9	65.6	33.8	57.2	3.2
Mamba-2 780M	0	**4.9**	**63.4**	**55.8**	71.7	61.1	30.6	**59.2**	–
	1	6.6	55.2	54.4	72.7	64.2	34.0	57.6	2.5
	3	7.8	52.7	54.9	**73.5**	65.0	**34.6**	57.8	**3.6**
	5	8.6	52.8	54.8	73.4	64.6	34.0	58.0	3.1
Pythia 1B	0	7.7	56.6	47.3	70.8	57.1	26.7	53.4	–
	1	8.8	52.0	47.4	70.7	57.5	28.8	53.6	1.8
	3	10.2	48.7	47.5	71.4	59.0	28.5	54.4	2.6
	5	10.6	48.8	47.4	71.5	58.9	28.4	53.0	2.0
Mamba 1.4B	0	**4.6**	**64.8**	59.3	74.3	65.2	35.1	62.3	–
	1	5.4	60.3	58.2	74.3	66.7	35.7	**62.8**	0.6
	3	6.1	59.3	58.4	74.1	67.4	36.6	61.8	1.0
	5	6.3	58.8	58.8	**74.5**	68.3	**37.0**	59.9	1.1
Mamba-2 1.3B	0	4.9	63.0	**60.1**	73.8	64.0	34.8	61.3	–
	1	6.1	58.2	59.2	74.2	67.0	35.0	60.1	0.5
	3	7.0	56.6	59.4	73.7	67.8	36.6	59.9	1.5
	5	7.2	56.5	59.9	73.5	**68.5**	36.7	60.7	2.2
Pythia 1.4B	0	5.2	63.6	52.9	71.1	61.2	30.3	58.2	–
	1	6.2	57.4	52.7	71.7	62.2	30.6	56.9	0.2
	3	7.0	56.1	53.1	71.1	64.5	32.8	56.8	2.3
	5	7.1	55.5	53.3	71.2	63.8	33.5	57.5	**2.9**
Mamba 2.8B	0	4.0	67.7	66.4	75.6	68.4	36.6	64.2	–
	1	4.8	63.3	65.9	76.2	70.9	39.4	64.6	2.4
	3	5.3	62.1	65.7	75.8	71.3	39.1	65.4	2.4
	5	5.4	61.9	66.2	77.2	71.4	40.4	66.1	3.9
Mamba-2 2.7B	0	**3.8**	**68.4**	**67.5**	76.0	69.5	38.3	65.3	–
	1	4.5	63.8	66.7	76.0	71.8	41.5	**67.1**	2.6
	3	5.0	62.3	67.3	76.2	**73.3**	44.4	66.0	4.5
	5	5.3	61.8	67.4	**76.4**	72.4	**44.5**	65.0	**4.1**
	0	5.0	64.7	59.3	74.0	64.7	33.3	59.2	–

E.1 Hardware throughput and memory-utilization improvements given PEFT and MPFT

With stable dynamics and observed divergences smaller than comparable Transformers, we show that MPFT and PEFT may be used to significantly increase GPU-training throughput for Mamba SSMs. To demonstrate such improvements, we utilize the previous fine-tuning settings for the Alpaca dataset. However, we now adjust the batch size to maximize throughput per MPFT and PEFT configuration.

For each MPFT and PEFT configuration, the *average tokens-per-second* (ATPS) is calculated as the total tokens used for fine-tuning divided by total training time, and the *maximum memory-per-token* (MMPT) is calculated as the maximum GPU memory utilization incurred (over the entire fine-tuning run) divided by the total number of tokens in each mini-batch. Results are plotted in Figure 4.

Both throughput and memory utilization improve as the number of Mamba parameters increases in Figure 4. **Compared to the full-precision full fine-tuning of `Mamba 790M`** (the largest model supported by an `A10G`'s memory capacity), evaluated **MPFT and PEFT combinations result in an average 2.15 times more training tokens-per-second while reducing per-token memory utilization by an average 62.7%**. Across all model sizes, evaluated MPFT and PEFT combinations result in an average 1.74 times more training tokens-per-second while reducing per-token memory utilization by an average 47.2% compared to respective full-precision fine-tuned runs. Furthermore, while full fine-tuning is no longer possible on a single `A10G` for Mamba models greater than 790 million parameters, MPFT and PEFT allow training Mamba models up to 2.8 billion parameters on GPUs with as little as 24 GB onboard memory.

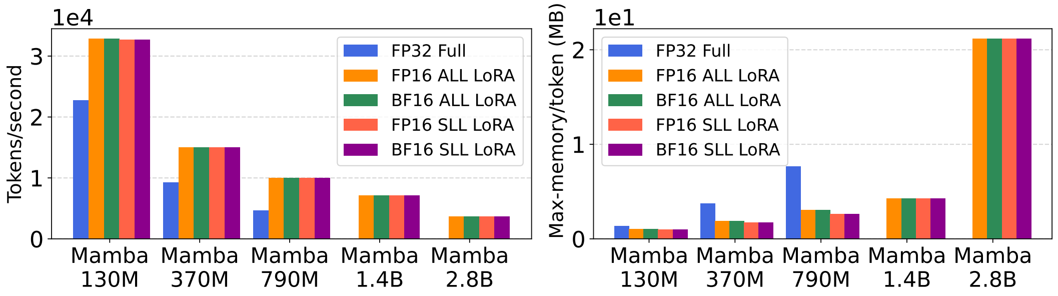

(a) Average tokens-per-second ↑.

(b) Maximum memory-per-token ↓.

Figure 4: Timing and memory usage calculated Mamba model-sizes and PEFT combinations. Each model was trained using the Alpaca dataset dataset for three epochs and maximum sequence length 512. For each PEFT combination, the batch size was tuned to maximize GPU occupancy. Full fine-tuning exceeds available GPU memory (24 GB) for models greater than 790 million parameters.

E.2 LoRA-layer robustness of Mamba models

We next show that carefully targeting specific Mamba layers (Theorem 3) can lead to more effective learning. For PEFT via LoRA, we thus explore the impact of targeting $\mathbf{W}$ (i.e., the linear weight storing the majority of time-varying SSM parameters) on performance.

Using OpenHermes and the training recipe described in Section 3 (with `BF16`), we instruction tune Mamba-2 models using LoRA by both adapting $\mathbf{W}$ and adapting all linear layers other than $\mathbf{W}$. Zero-shot performance is evaluated using five standard natural language benchmarks: HellaSwag (Zellers et al., 2019), PIQA (Bisk et al., 2020), Arc-E (Clark et al., 2018), Arc-C (Clark et al., 2018), and WinoGrande (Sakaguchi et al., 2021). As shown in Table 4, PEFT with only $\mathbf{W}$ targeted near uniformly results in better performance than targeting other layers, with the former outperforming the latter on 32 out of 35 natural language tasks.

F ICL as an emergent ability of Mamba SSMs

We study the emergent behavior (as a function of model size) of Mamba/Mamba-2 SSMs' ICL abilities on natural language tasks by comparing to a larger number of Transformer-based LLMs of varying sizes.

Table 4: Zero-shot performance for instruction tuned Mamba-2 models where: denotes the large memory buffer **W** containing the majority of temporal variables (described in Section 2.2) is targeted for LoRA adaptation, and denotes **W** is not adapted. The top-performance for each task per model is highlighted in bold .

Model	**W** targeted?	LAMBADA ppl ↓	LAMBADA acc ↑	HellaSwag acc ↑	PIQA acc ↑	Arc-E acc ↑	Arc-C acc ↑	WinoGrande acc ↑
Mamba-2 130M		**15.37**	**45.26**	**35.4**	**65.0**	**47.9**	**24.9**	52.2
		16.95	43.3	35.2	64.9	47.5	24.1	52.2
Mamba-2 370M		**8.03**	**54.2**	**46.9**	69.5	53.5	**27.7**	**57.1**
		8.50	53.7	46.6	**70.7**	**54.8**	26.8	55.6
Mamba-2 780M		**5.79**	61.6	**55.1**	72.0	61.1	29.2	60.1
		5.86	61.6	54.9	72.0	61.0	28.4	**60.2**
Mamba-2 1.3B		**4.54**	**65.7**	**60.9**	**73.7**	**66.2**	**34.6**	**61.8**
		5.05	65.4	59.8	73.4	64.1	33.1	61.1
Mamba-2 2.7B		**4.05**	**69.6**	**66.7**	**76.5**	**70.0**	**36.8**	**64.6**
		4.10	69.6	66.6	76.4	69.5	36.3	63.9

We compare to `OpenELM` (Mehta et al., 2024) (sizes `270M`, `450M`, and `1.1B`), `TinyLlama 1.1B` (Zhang et al., 2024), and `OLMo 1.2B` (Groeneveld et al., 2024). To limit the emergent effects on both parameter size and pretraining token counts, we did not evaluate models greater than 2.8 billion parameters and chose open-source checkpoints as close as possible to the 300 billion total pretraining tokens used for Mamba, Mamba-2, and Pythia models. Thus, pretraining token counts for OpenELM, TinyLlama, and OLMo models were 429 billion, 503 billion, and 336 billion, respectively. We note this potentially biases ICL performance in favor of the newly evaluated Transformer-based LLMs, and that direct comparisons between Mamba, Mamba-2, and Pythia are the most fair (as these three classes of models were all pretrained on the same dataset for the same number of total pretraining tokens).

We repeat the experiments from Figure 3, where we evaluate the pretrained and instruction tuned ICL capabilities of all models. To understand the critical role of parameter counts, we group all models into two classes: LLMs containing 450 million parameters or less, and LLMs containing greater than 450 million parameters. ICL performance measured by AIPSS is displayed in Figure 5.

From Figure 5, it is clear that pretrained SSMs and Transformers of parameter counts 270 million and less display slight or detrimental ICL abilities (i.e., few-shot performance is worse than zero-shot). For models of greater than 450 million parameters, the majority of SSMs and Transformers display positive ICL abilities, with `Mamba 1.4B` being an outlier in terms of poor performance. With the exception of TinyLlama at 1-shot performance and `Mamba-2 2.7B` for 3- and 5-shot performance, the majority of other pretrained models cluster together.

Instruction tuning greatly smooths ICL performance across both parameter classes. While instruction tuned SSMs and Transformers of 160 million parameters or fewer continue to display slight or detrimental ICL abilities, all parameters of 270 million and greater show positive ICL abilities. For instruction tuned models of greater than 450 million parameters, all SSMs and Transformers show positive ICL abilities, with `Mamba-2 2.7B` greatly outperforming all other models (both SSM and Transformer) in this class.

Thus, in terms of ICL as a function of SSM model size, while no clear trend presents itself for pretrained models, ICL emerges for instruction tuned Mamba and Mamba-2 SSMs of size 370 million and greater.

G Expanded divergence results: Alpaca and LIMA fine-tuning, MMLU and Winogrande benchmarks, Mean and Standard Deviation divergences

We extend the non-divergent Mamba fine-tuning results from Section 3. Recall that the following MPFT and PEFT configurations are considered to fine-tune each considered LLM:

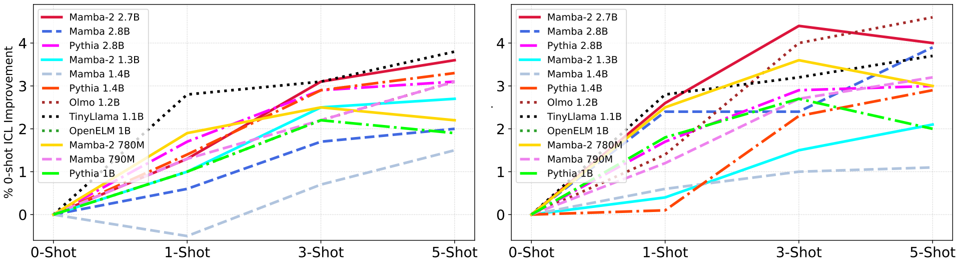

(a) 450M < Parameter total, Pretrained (b) 450M < Parameter total, `ALL LoRA`

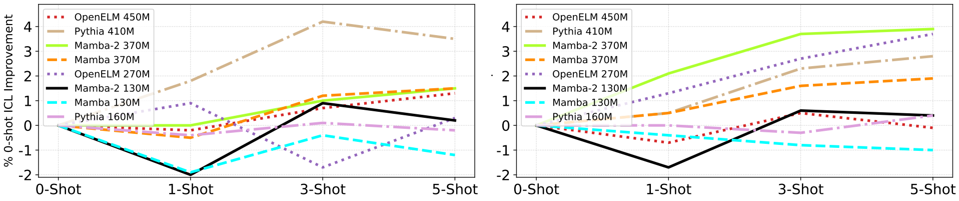

(c) Parameter total ⩽ 450M, Pretrained (d) Parameter total ⩽ 450M, `ALL LoRA`

Figure 5: Instruction tuning improves Mamba-2 ICL performance past Transformer LLMs. `ALL LoRA` models were instruction fine-tuned on the OpenHermes dataset for one epoch. Performance is reported as the average improvement percentage of {1, 3, 5}-shot versus 0-shot over five standard natural language benchmarks: HellaSwag, PIQA, Arc-E, Arc-C, and WinoGrande.

1. Full fine-tuning in `FP32`
2. Full fine-tuning in `FP16`
3. Full fine-tuning in `BF16`
4. `ALL LoRA`fine-tuning in `FP32`
5. `ALL LoRA`fine-tuning in `FP16`
6. `ALL LoRA`fine-tuning in `BF16`
7. `SLL LoRA`fine-tuning in `FP32`
8. `SLL LoRA`fine-tuning in `FP16`
9. `SLL LoRA`fine-tuning in `BF16`

In addition to the `Alpaca` dataset (Taori et al., 2023), we also fine-tune all models using the `LIMA` dataset (Zhou et al., 2024). Models are trained using `LIMA` for 5 epochs, while all other settings follow the fine-tuning recipe used for `Alpaca` (described in Appendix E).

For natural language benchmarks, in addition to MMLU, we evaluate each fine-tuned model using Winogrande (Sakaguchi et al., 2021). Recall that, for each benchmark, divergence between a mixed-precision fine-tuned model is measured between its full-precision counterpart and averaged over {0, 1, 3, 5}-shot performance. In addition to the average divergence, we also include the standard deviation of divergence. Thus, **in total, 144 LLMs were fine-tuned, 576 MMLU evaluations were conducted, and 576 Winogrande evaluations were conducted.**

Figure G displays results for `Alpaca` and MMLU, Figure G displays results for `Alpaca` and Winogrande, Figure G displays results for `LIMA` and MMLU, Figure G displays results for `LIMA` and Winogrande. Summary statistics for all experiments are presented in Table G. While OpenELM exhibits large deviation spikes for both `Alpaca` benchmark evaluations–and Pythia exhibits large deviation spikes for all four evaluations–**Mamba**

does not exhibit a single large deviation spike on any benchmark for all considered model sizes and MPFT/PEFT configurations (i.e., 18 total configurations excluding the full-precision baselines). Furthermore, Mamba models are significantly more stable for MPFT/PEFT compared to Transformer-based LLMs. E.g., **for MMLU evaluations, `Alpaca` fine-tuning with Mamba models is an average 2.6 times smaller in mean divergence than both Pythia and OpenELM models, while `LIMA` fine-tuning with Mamba models is an average 7 and 3.25 times smaller in mean divergence than Pythia and OpenELM models, respectively**.

Table 5: Summary of divergence results for `Alpaca` and `LIMA` fine-tuning datasets, MMLU and Winogrande benchmarks, and Mamba, OpenELM, and Pythia models. For each deviation summary statistic per fine-tuning dataset and benchmark, the lowest deviation is highlighted in bold.

(Fine-tuning dataset), Benchmark	Architecture	Large deviation spikes ↓	Avg mean divergence ↓	Std mean divergence ↓
(`Alpaca`, MMLU)	Pythia	1	0.37	0.41
	OpenELM	1	0.37	0.32
	Mamba	**0**	**0.14**	**0.08**
(`Alpaca`, Winogrande)	Pythia	4	0.72	0.58
	OpenELM	3	0.59	0.37
	Mamba	**0**	**0.25**	**0.09**
(`LIMA`, MMLU)	Pythia	1	0.28	0.34
	OpenELM	**0**	0.13	0.15
	Mamba	**0**	**0.04**	**0.03**
(`LIMA`, Winogrande)	Pythia	3	0.45	0.45
	OpenELM	**0**	0.36	0.18
	Mamba	**0**	**0.11**	**0.12**

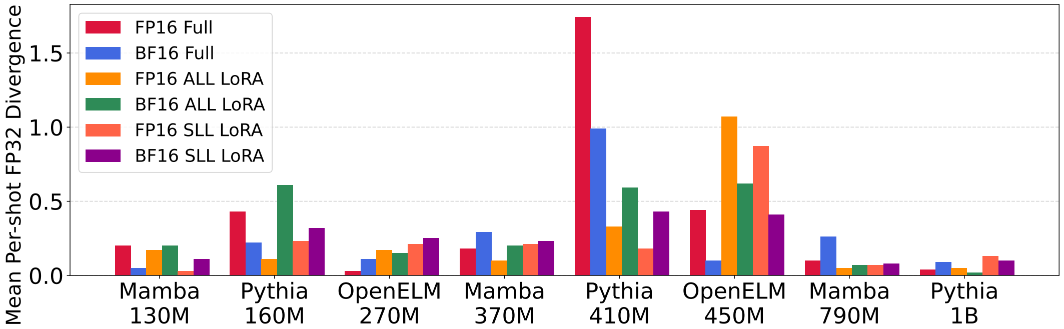

(a) Mean full-precision (`FP32`) divergence in MMLU performance.

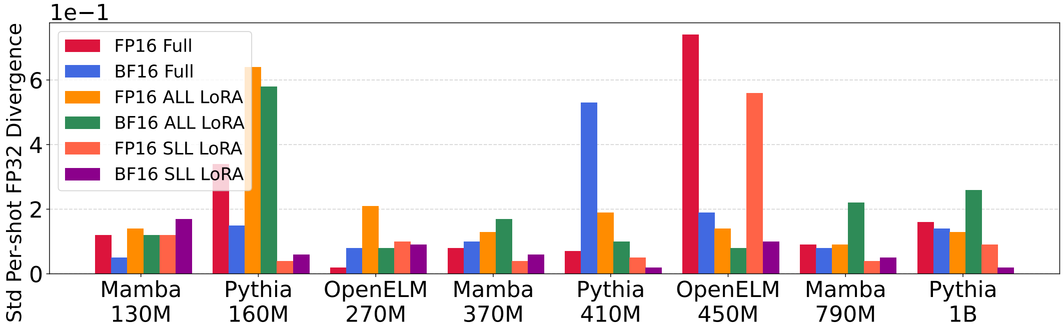

(b) Standard deviation (std) full-precision (`FP32`) divergence in MMLU performance.

Figure 6: **Alpaca fine-tuning, MMLU evaluation.** Mamba, Pythia, and OpenELM models are fine-tuned over the `Alpaca` dataset using different combinations of MPFT and PEFT. Full fine-tuning (i.e., no PEFT adapters) is denoted as `Full`.

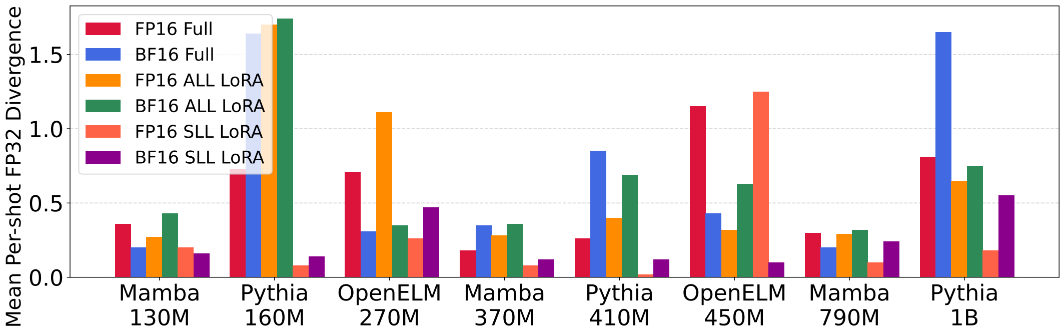

(a) Mean full-precision (`FP32`) divergence in Winogrande performance.

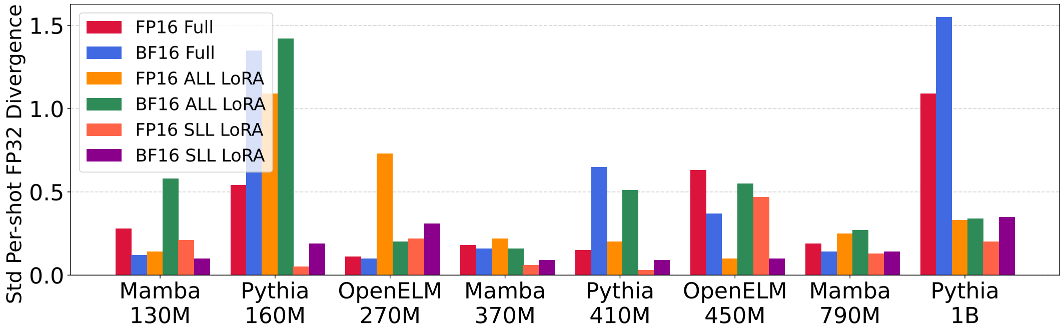

(b) Standard deviation (std) full-precision (`FP32`) divergence in Winogrande performance.

Figure 7: **Alpaca fine-tuning, Winogrande evaluation.** Mamba, Pythia, and OpenELM models are fine-tuned over the `Alpaca` dataset using different combinations of MPFT and PEFT. Full fine-tuning (i.e., no PEFT adapters) is denoted as `Full`.

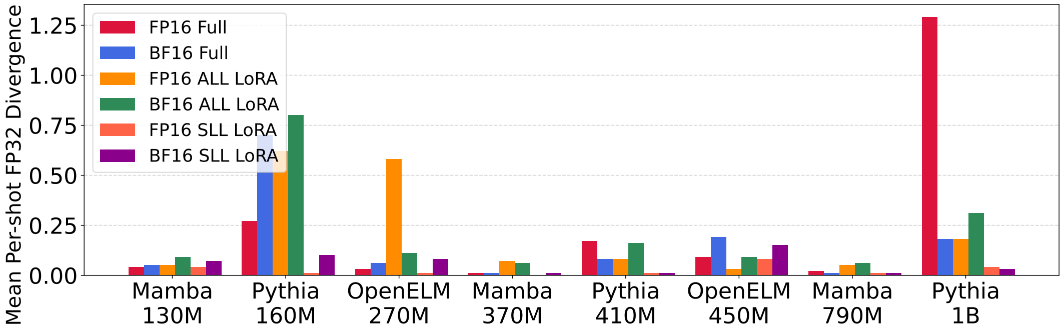

(a) Mean full-precision (`FP32`) divergence in MMLU performance.

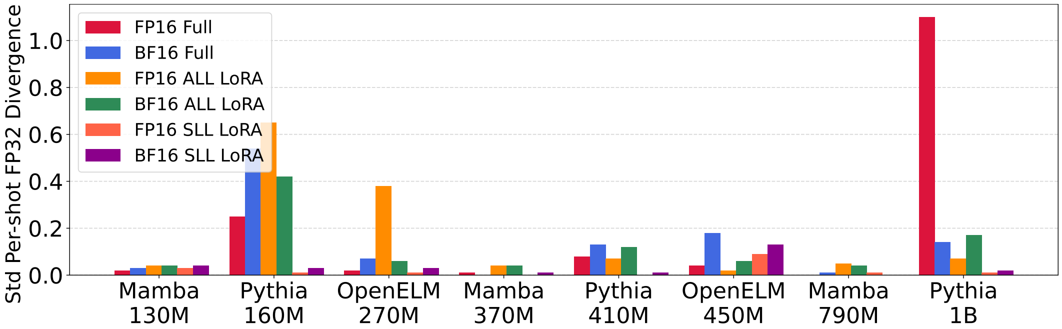

(b) Standard deviation (std) full-precision (`FP32`) divergence in MMLU performance.

Figure 8: **LIMA fine-tuning, MMLU evaluation.** Mamba, Pythia, and OpenELM models are fine-tuned over the `LIMA` dataset using different combinations of MPFT and PEFT. Full fine-tuning (i.e., no PEFT adapters) is denoted as `Full`.

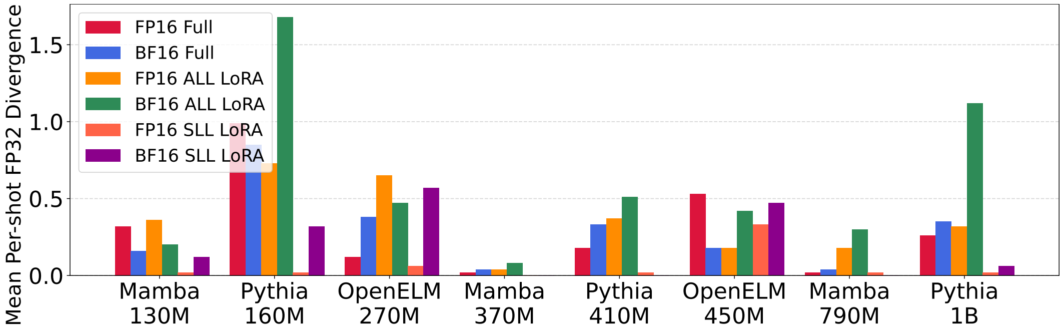

(a) Mean full-precision (`FP32`) divergence in Winogrande performance.

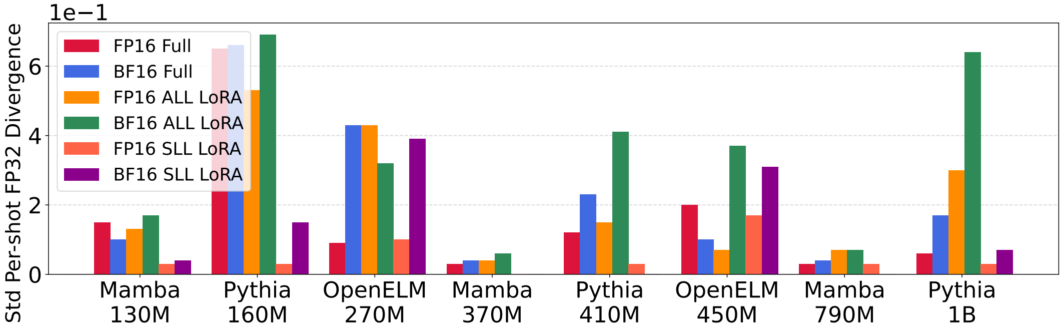

(b) Standard deviation (std) full-precision (`FP32`) divergence in Winogrande performance.

Figure 9: **LIMA fine-tuning, Winogrande evaluation.** Mamba, Pythia, and OpenELM models are fine-tuned over the `LIMA` dataset using different combinations of MPFT and PEFT. Full fine-tuning (i.e., no PEFT adapters) is denoted as `Full`.